

 **DOR: 20.1001.1.27170314.2022.11.1.5.1**

Research Paper

Fabrication of Various Dimple Shapes and Arrays on a Hypereutectic Al-Si Alloy Using a Turning Process

Jaharah A. Ghani^{1*}, Faarih Farhan Mohd Nasir¹, Mohd Nor Azam bin Mohd Dali², Wan Fathul Hakim W. Zamri¹, Mohd Shahir Kasim³, Che Hassan Che Haron¹

¹Department of Mechanical and Material Engineering, Faculty of Engineering and Built Environment, Universiti Kebangsaan Malaysia, 43600 Bangi, Selangor, Malaysia

²Politeknik Ungku Omar, Jalan Raja Musa Mahadi, 31400 Ipoh, Perak, Malaysia

³Faculty of Manufacturing Engineering, Technical University of Malaysia, Durian Tunggal, Malaysia

*Email of Corresponding Author: jaharahghani@ukm.edu.my

Received: April 13, 2022; Accepted: June 10, 2022

Abstract

A hypereutectic Al-Si alloy piston has great potential for use in the automotive industry, especially for engine components, due to its lightweight, excellent castability, good thermal conductivity, high strength and excellent corrosion resistance. The silicon content in the A390 is between 17-18%. This article presents various shapes of dimples that can be fabricated on a cylindrical shape part of A390 using the turning process with aid of dynamic assisted tooling (DATT). To minimize the number of the experiment, the Taguchi method, with an L8 orthogonal array, was used to accommodate two different sets of seven parameters used in the fabrication of dimpled structures, i.e. cutting speed of 2-9 m/min, feed rate of 0.4-0.6 mm/rev, DOC of 0.05-0.01 mm, frequency of 15-28 Hertz, the amplitude of 1-3 mm, using two different cutting tool i) rake angle of +4° and -8.5°, relief angle of 4° and 7°, and nose radius of 0.4 and 0.8 mm, ii) Rake angle of +9° and -20°, and relief angle of +7° and +17°, and nose radius 8 mm. By using these turning parameters, 3 dimple shapes were produced; spherical, short drop and long drop shapes, with almost square and hexagonal arrays.

Keywords

Dimple Shapes, Al-Si Alloy, Turning Process, DATT

1. Introduction

Fuel efficiency and high engine performance are major challenges for vehicle automotive producers in achieving their desired targets. Problems involving heavy engine components, and friction and wear on sliding components are closely related to fuel efficiency and performance. The heaviest components are in the engine, and Dhingra & Das [1] stated that one good way of reducing the weight of these components is by replacing cast iron with aluminium. According to Hirsch [2], aluminium is a light material and it can reduce the weight by 50 % in most applications. Due to its lightweight, excellent resistance to abrasion and corrosion, low coefficient of thermal expansion and high strength, aluminium has become the material of the first choice in the piston industry, according to Zeren. [3]. Aluminium-Si alloy is divided into 3 parts, based on the percentage of silicon, i.e. 12-13 % of silicon is classified as eutectic, below 12 % is classified as hypoeutectic, and above 14 % is classified as

hypereutectic Al-Si alloy, as per Lee [4]. According to Holmberg et al. [5], the piston assembly, which makes up about 45 % of the engine components, is the main contributor to friction and wear in an engine system. There are 4 methods for minimizing friction and wear, namely by coating the engine components, surface texturing of the engine components, lubrication, and rolling resistance in the tyres, as per Holmberg et al. [6].

According to Bruzzone et al. [7], a lot of discussions about the correlation properties and the functions of a surface have led to the discovery of the distribution of micro dimples on the surface that acts as a reservoir and provide lubrication to reduce friction by 30%. This fact was also supported by Xiaolei et al. [8], who found that micro-textured surfaces, such as dimples or grooves, are capable of maintaining lubrication. According to Basnyat et al. [9] and Voevodin et al. [10], lubrication by micro dimples will enhance the tribology of mechanical parts since the dimples act as reservoirs on the surface.

Although laser surface texturing (LST) and etching process are famously used for surface texture because of advanced technology, high production speed and low production time, these processes are expensive and non-eco-friendly processes [11-12]. Therefore, the turning process was used in this research because of its advantages such as low cost, minimum set-up time and being environmentally friendly, which are suitable for mass production for fabricating dimple structures. The Taguchi method of applying an orthogonal array design has the advantage of lowering the number of experiments required while still being able to produce the same results as the other methods, thereby reducing the experimental time and costs, according to Fratila and Caizar [13]. This study focused on the fabrication of various shapes and arrays of dimple structures on a hypereutectic Al-Si alloy piston by considering all the seven parameters in minimizing friction and wear.

2. Methodology

Experiments were conducted using a CNC Colchester Tornado lathe with assisted tooling that was developed in-house to generate vibrations on the cutting tool. Given below are the cutting parameters (Table 1), which consist of seven parameters for the cutting tool (i) and (ii).

Table 1. Two levels of cutting parameters

Factors	Cutting tool (i)		Cutting tool (ii)	
	Levels		Levels	
	1	2	1	2
Frequency, f_q (Hz)	15	25	1	2
Cutting Speed, V_c (m/min)	7	9	25	28
Feed Rate, f (mm/rev)	0.4	0.6	9	2
Depth of Cut, ap (mm)	0.01	0.5	0.4	0.6
Amplitude, amp (mm)	1	3	0.05	0.1
Rake angle and Relief angle (Degree)	-8.5° & 7°	-8.5° & 7°	1	3
Nose Radius, r_ϵ (Degree)	0.4	0.8	-20° & 17°	+9° & 7°

3. Results and discussion

Table 2 shows the results of the experiments that were conducted for the tool (i). Based on observations using an Olympus microscope at a magnification of 6.7x and a 3D profilometer, 3 shapes and 3 uniform arrays were produced, as shown in Figures 1 to 3.

Table 2. Experimental Results (L_8)

Exp. L_8 (2^7)	Width (μm)		Length (μm)		Depth (μm)	
	(S1)	(S2)	(S1)	(S2)	(S1)	(S2)
1	310	160	2740	2300	39.9	68.6
2	610	590	1500	1510	158.6	130.7
3	450	260	3730	2130	39.9	67.3
4	520	280	1750	1010	182	143.6
5	550	340	1930	1210	97.6	127
6	220	360	2430	1750	78.9	110.8
7	270	180	1500	1020	56	74.4
8	440	460	1320	1590	104.7	58.1

Note: Sample 1 (S1) and Sample 2 (S2)

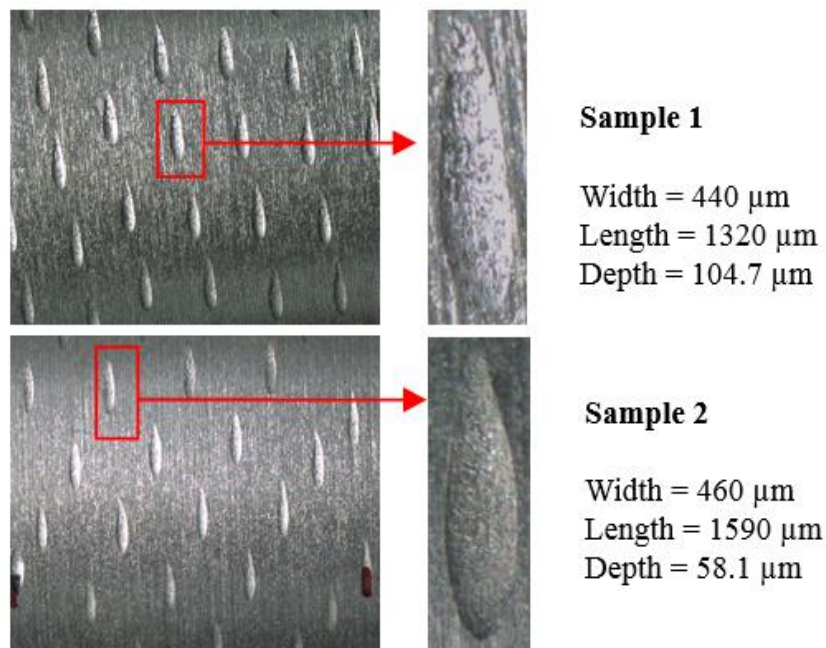


Figure 1. Dimple arrays and shapes for a cutting speed of 9 m/min, feed rate of 0.6 mm/rev, depth of cut of 0.01 mm, frequency of 25 Hertz, the amplitude of 1 mm, rake angle of -8.5° , relief angle of 7° and nose radius of 0.8 mm

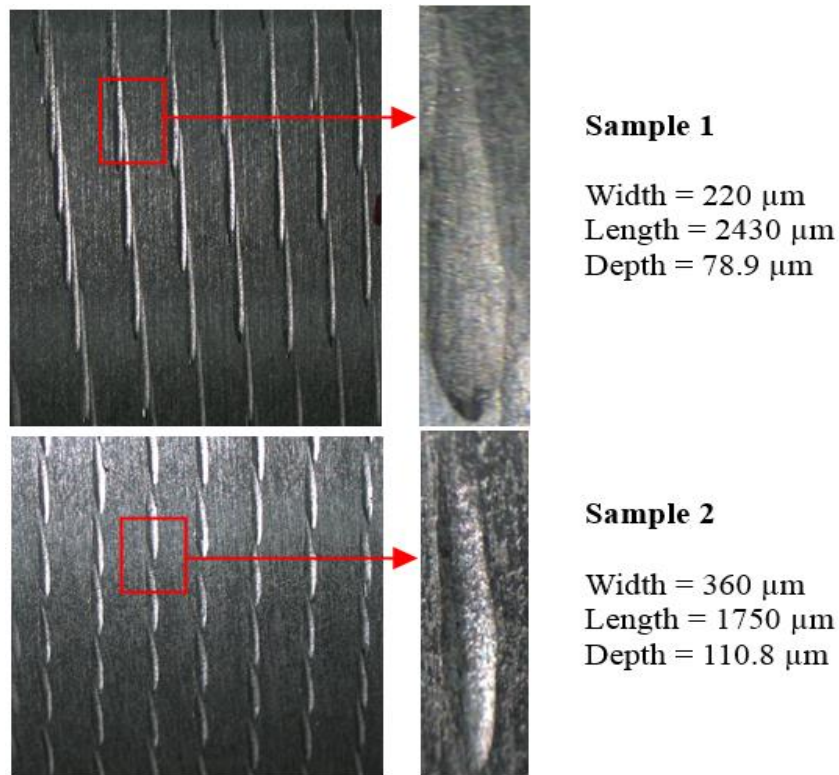


Figure 2. Dimple arrays and shapes for cutting speed of 9 m/min, feed rate of 0.4 mm/rev, depth of cut of 0.05 mm, frequency of 25 Hertz, the amplitude of 1 mm, rake angle of $+4^\circ$, relief angle of 4°

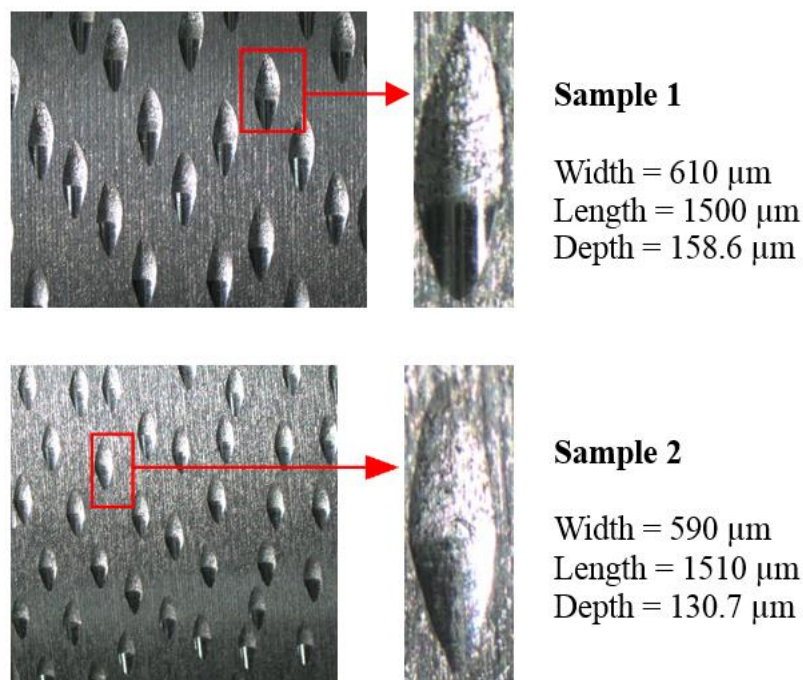


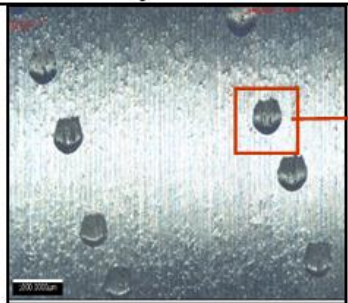
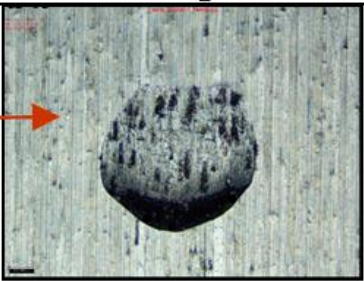
Figure 3. Dimple arrays and shapes for cutting speed of 7 m/min, feed rate of 0.4 mm/rev, depth of cut of 0.01 mm, frequency of 25 Hertz, the amplitude of 3 mm, rake angle of $+4^\circ$, relief angle of 4° and nose radius of 0.8 mm

Table 2 shows the results obtained using the cutting tool (ii).

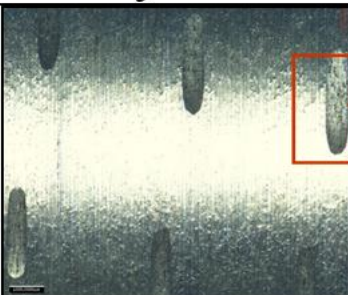
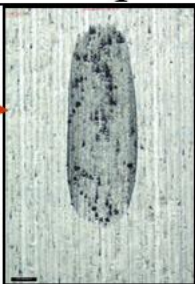
Table 2. The results obtained using the cutting tool (ii)

No. Exp	Average Width (μm)	Average Length (μm)	Average Depth (μm)
1	565.15	517.03	30.88
2	895.95	826.26	83.67
3	961.39	3163.13	84.19
4	646.26	2661.36	23.60
5	1039.19	3927.61	124.87
6	869.80	2781.43	58.80
7	787.27	885.98	87.05
8	829.22	1026.65	110.70

Figures 4 and 5 show two selected shapes using the cutting tool (ii).

Array Pattern	Dimple	Dimensions (μm)
		Width = 565 Length = 517 Depth = 31

Figures 4. $V_c = 2$ m/min, $f = 0.5$ mm/rev, $a_p = 0.05$ mm, $a_{mp} = 1$ mm, $f_q = 25$ Hz and (c) short drop dimple structure; (Experiment 1)

Array Pattern	Dimple	Dimensions (μm)
		Width = 646 Length = 2661 Depth = 23

Figures 5. $V_c = 9$ m/min, $f = 0.4$ mm/rev, $a_p = 0.05$ mm, $a_{mp} = 1$ mm, $f_q = 25$ Hz and (c) long drop dimple structure; (Experiment 4)

The observation of the dimple shapes produce using a turning machine aided with a DATT can be benefited by the user in various industries, particularly automotive. Based on a review by Nasir et al. [14], they stated that having an elliptical shape dimpled surface (short drop and long drop) has the advantage in a lubrication environment for reducing the coefficient of friction. A small dimple structure can retain lubricant while a large dimple structure can produce hydrodynamic pressure. Ellipse shapes have the greatest friction reduction effect compared to other dimple shapes (circle and

square) due to having the largest converging wedge that simply develops lubricant film between two surfaces [15].

4. Conclusion

Based on the dimple shapes and arrays that were derived, the shapes, particularly the width, length and depth were still within the acceptable range of previous studies, and continuous upgrading needs to be done by optimizing the machining parameters so that the depth of the dimple structure can be further reduced below 100 μm . Previous researchers fixed the dimple geometry at a diameter of 20 μm -4 mm and a depth of 200 nm-100 μm to affect the tribological performance. On the other hand, the arrays can be improved to obtain more precise square, hexagonal and triangular shapes through the optimization of the machining parameters used.

5. References

- [1] Dhingra, R. and Das, S. 2014. Life cycle energy and environmental evaluation of downsized vs. lightweight material automotive engines. *Journal of Cleaner Production* 85:347-358.
- [2] Hirsch, J. 2014. Recent development in aluminium for automotive application. *Transactions of Nonferrous Metal Society of China*, 24:1995-2002.
- [3] Zeren, M. 2007. The effect of heat treatment on aluminium-based piston alloys. *Material and Design*. 28:2511-2517.
- [4] Lee, J. A. 2003. Cast Aluminium Alloy for High Temperature Applications. The 132nd TMS Annual Meeting & Exhibition San Diego Convention Centre, San Diego, CA.
- [5] Holmberg, K., Andersson, P. and Erdemir, A. 2012. Global energy consumption due to friction in passenger cars. *Tribology International*. 47:221-234.
- [6] Holmberg, K., Andersson, P. and Nylund, N.O. Makela, K. and Erdemir, A. 2014. Global energy consumption due to friction in trucks and buses. *Tribology International*. 78:94-114.
- [7] Bruzzone, A. A.G., Costa, H.L., Lonardo, P.M. and Lucca, D. A. 2008. Advances in engineering surfaces for functional performance. *CIRP Annals: Manufacturing Technology*. 57:750 -769.
- [8] Xiaolei, W., Wei, L., Fei, Z. and Di, Z. 2009. Preliminary investigation of the effect of dimple size on friction in line contact. *Tribology International*. 42:1118 – 1123.
- [9] Basnyat, P., Luster, B., Muratore. C., Voevodin, A.A., Haasch, R. and Zakeri, R. 2008. Surface Texturing for adaptive solid lubrication. *Surface & Coatings Technology*. 203:73-9.
- [10] Voevodin, A.A., and Zabinski, J.S. 2006. Laser surface texturing for adaptive solid lubrication. *Wear*. 261:1285-92.
- [11] Gachot, C., Rosenkranz, A., Hsu, S.M. and Costa, H.L. 2017. A critical assessment of surface texturing for friction and wear improvement. *Wear*. 372 (3):21-41.
- [12] Rosenkranz, A., Grützmaker, P.G., Gachot, C. and Costa, H.L. 2019. Surface texturing in machine elements– a critical discussion for rolling and sliding contacts, *Advanced Engineering Materials*. 21(8):190-194.
- [13] Fratila, D. and Caizar, C. 2011. Application of Taguchi method to selection of optimal lubrication and cutting condition in face milling of AlMg3. *Journal of Cleaner Production*, 19: 640-645.

- [14] Nasir, F.F.M., Ghani, J.A., Zamri, W.F.H.W. and Kasim, M.S. 2019. State-of-the-art surface texturing and methods for tribological performance, *World Review of Science, Technology and Sustainable Development*. 15(4):330-357.
- [15] Yu, H., Deng, H., Huang, W. and Wang, X. 2011. The effect of dimple shapes on friction of parallel surfaces, *Proceedings of the Institution of Mechanical Engineers, Part J: Journal of Engineering Tribology*. 225 (8):693-703.